Pergamon

0301-9322(94)E0034-G

Int. J. Multiphase Flow Vol. 20, No. 5, pp. 885–899, 1994

0301-9322/94 $7.00 + 0.00

TWO-PHASE (AIR–WATER) FLOW PATTERNS AND PRESSURE DROP IN THE PRESENCE OF HELICAL WIRE RIBS

J. WEISMAN, J. LAN and P. DISIMILE
College of Engineering, University of Cincinnati, Cincinnati, OH 45221-0072, U.S.A.

(Received 30 August 1993; in revised form 15 March 1994)

Abstract—An examination of two-phase flow patterns and pressure drops in single and double helically ribbed circular tubes has been performed. The present studies were conducted in both a 2.54 and 5.1 cm circular tube using low pressure air–water mixtures maintained at room temperature. Ribs of a circular cross section were utilized with heights of 0.32, 0.64 and 1.27 cm. Helical twist ratios of 1.2, 2.1, 2.3 and 2.5 were used. Results indicate that swirling annular flow is seen at low qualities once a minimum liquid velocity is exceeded. Therefore, it is expected that an enhancement of the critical heat flux would also occur above this minimum liquid velocity. Dimensionless correlations have been devised for the various flow pattern transitions which were observed.

Key Words: flow pattern, two-phase flow, gas–liquid, flow regime map, helical ribs

INTRODUCTION

One of the widely used approaches for enhancing forced convection single-phase and boiling heat transfer inside tubes is the installation of internal helical ribs. Ribbed tubes have been shown to increase the critical heat flux significantly and they are now commonly used in industrial boilers (Watson *et al.* 1974).

The swirling flow produced by helical ribs has the beneficial effect of forcing the liquid to the tube wall and carrying the vapor to the tube center. There is, however, very limited information on the conditions under which the desired swirling flow is obtained. Prior to this investigation, the limited work of Zarnett & Charles (1969) indicated that, at low and moderate qualities, swirling flow was not obtained until a critical liquid superficial velocity was reached. These investigators examined air–water two-phase flow in a 1.9 cm (3/4 inch) i.d. tube at atmosphere pressure. The ribs were provided by a hellically coiled wire with a 0.81 cm^2 cross section. They used pitch to tube diameter ratios of 1.6 and 2.8. Although Zarnett & Charles examined two geometries, they found little difference in the flow patterns seen. They therefore reported only a single flow pattern map. A replot of this flow pattern map is shown in figure 1. It is clear from their descriptions that swirling flow was only obtained in the semiannular and annular regions.

No study of two-phase flow patterns in addition to that of Zarnett & Charles (1969) was known to the authors prior to this work. It was therefore decided that a more comprehensive examination of two-phase flow patterns and pressure drop in ribbed tubes would be desirable. In this study, all ribs were produced by the insertion of a helical coil or coils of round wires. The wires fit tightly against the inner diameter of the tube.

EXPERIMENTAL PROGRAM

Flow patterns and pressure drop studies were carried out in horizontal tubes with air and water at room temperature and pressures close to atmospheric. The experiments were carried out in the University of Cincinnati flow pattern apparatus previously described by Weisman *et al.* (1979).

The apparatus basically consists of a simple tee in which the air and water mixed, a set of horizontal transparent tubes, an air–water separation tank, water recirculation pump and source of compressed air. Air from the compressor is mixed with the recirculated water in a horizontal

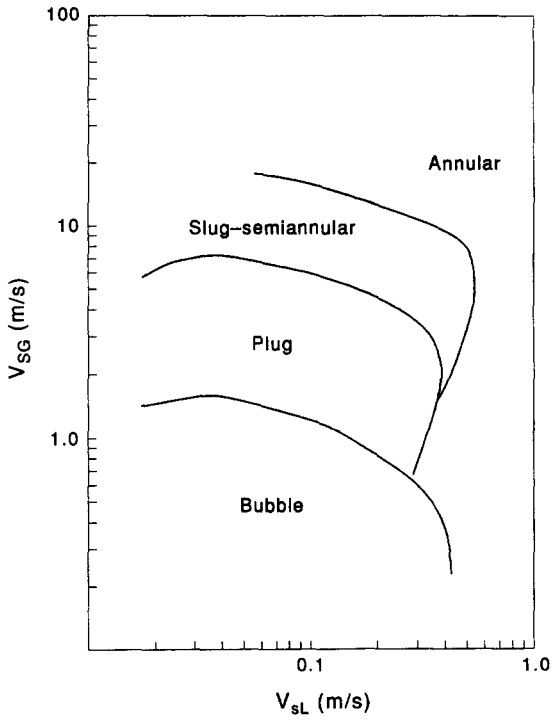

Figure 1. Flow pattern map of Zarnett & Charles (D = 1.9 cm, d = 0.32 cm, y = 0.79 and 1.4) square ribs.

tee. The two-phase mixture then flows through one of a set of three 7.1 m long transparent tubes. The mixture exiting the transparent test sections flows to the separation tank and the separated water is recirculated to the mixer inlet.

In the present tests of single coils, helical ribs were inserted in the first ~3 m of the test sections. In all cases, the helical ribs were produced from round wires and therefore the ribs had a circular cross section. Only a ~3 m length was used since difficulty was encountered in fabricating longer helices. The inlet portion of the test section was used since it was found that, if the outlet section were used, the empty tube flow patterns tended to persist and distort results. Flow pattern observations were made visually at the end of the helically ribbed section.

In the one test of a double helix, we were unable to fabricate a 3 m section with consistent wire spacing. A 1.85 m test length was therefore used. As before, the wires were inserted in the first portion of the test section. Since this test was carried out in the 2.54 m tube the helix length still provided an L/D ratio of over 70. This was believed to be satisfactory since visual flow pattern observations taken after an L/D of about 40 showed no change with position along the tube. This is consistent with earlier observations of two-phase flow pattern behavior in an empty tube (Weisman *et al.* 1979).

In addition to the visual flow pattern observations, axial pressure drops were also measured for both single and two-phase flows. The pressure measurements were made using a differential pressure transducer and purge water was provided prior to all measurements to make certain that the lines to the differential pressure transducer contained only water.

Tests were conducted in both 2.54 and 5.1 cm lines. Based on wire availability, and the desire to test wire to tube diameter ratios greater than those previously examined, wire diameter to tube diameter ratios of 1/4 and 1/8 were selected for testing. The helical twist ratio, given by "y" where

$$y = (\text{distance for } 180^\circ \text{ turn})/(\text{tube diameter}),$$

varied from 1.2 to 2.5. The foregoing definition of "y" was used to be consistent with the ratio which has been used for characterization of twisted tapes. Table 1 summarizes the geometrics examined in the present test as well as in the earlier experiments of Zarnett & Charles (1969).

Table 1. Helical rib geometries

Investigator	Tube dia (cm)	Rib height (cm)	Rib cross section	y	$P/2D$
Zarnett & Charles	1.9	0.32	square	0.79	0.79
Zarnett & Charles	1.9	0.32	square	1.4	1.4
Present study	5.1	1.27	circular	2.3	2.3
Present study	5.1	1.27	circular	1.2	1.2
Present study	5.1	0.64	circular	2.1	2.1
Present study	2.54	0.32	circular	2.5	2.5
Present study	2.54	0.32	circular	2.5	1.25

P = pitch = distance between adjacent wires.
D = tube diameter.

FLOW PATTERN STUDIES

The observed flow patterns were categorized following the approach used previously for flow patterns in empty tubes (Weisman *et al.* 1979; Weisman & Kang 1981). The flow pattern categories used for horizontal flow were:

(1) annular flow—liquid around outside of tube, central core of vapor or vapor and droplets
(2) dispersed flow—dispersion of bubbles in liquid or droplets in vapor with dispersed and continuous phase moving together
(3) intermittent flow—large plugs of vapor moving through the liquid or slugs of liquid periodically moving down tube
(4) bubbly flow—small bubbles of vapor moving through liquid
(5) separated flow—stratified or wavy flow (layer of liquid on bottom of tube with smooth or wavy interface).

This categorization differs slightly from that used by Zarnett & Charles (1969) since no "slug-semi-annular" region is used. In the present tests, the transition to annual flow was assumed to occur whenever the top of the tube remained wetted continuously. The semi-annular flow of Zarnett & Charles would be annular in the present sense.

All experimental investigators have noted that flow pattern transitions occur over a range of flows and that there is therefore some uncertainty in the exact location of the boundary. The flow pattern transitions observed in the present tests are therefore indicated by shaded bands in the flow pattern maps of figures 2 and 3. Although the flow pattern transition bands have been drawn following the five categories indicated previously, the symbols on the flow maps also differentiate between stratified and wavy flow. In the intermittent region, only slug flow was observed.

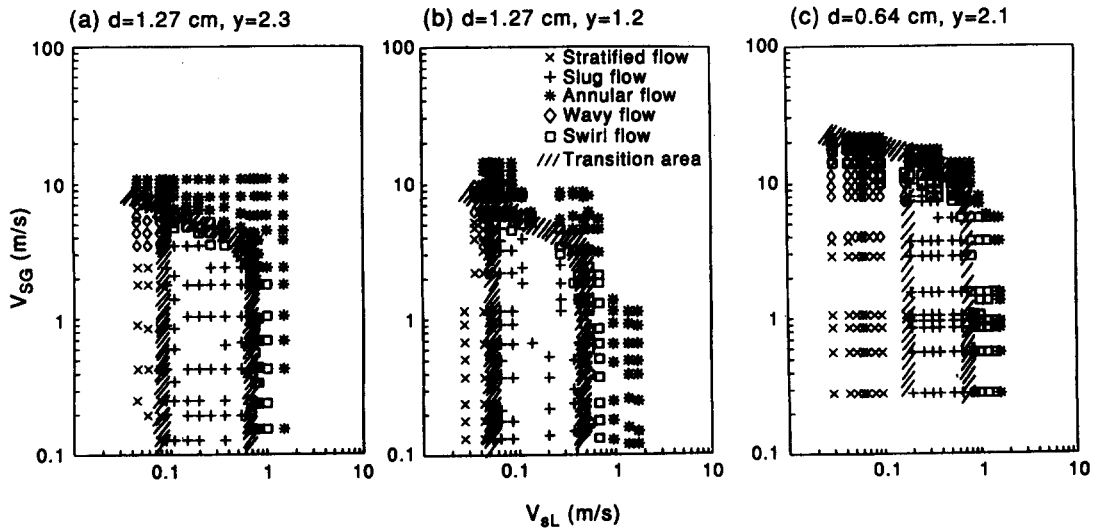

Figure 2. Flow pattern maps for the 5.1 cm tube (single helix).

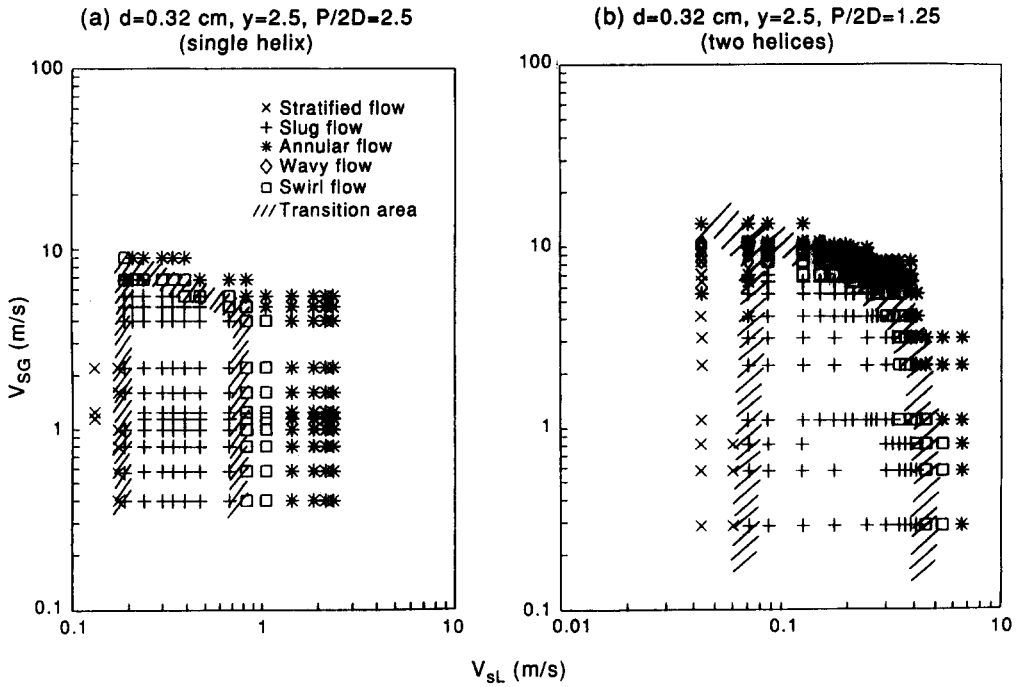

Figure 3. Flow pattern maps for the 2.55 cm tube.

The flow pattern observations of the present experiment are similar to those of Zarnett & Charles (1969) in respect to the disappearance of dispersed flow. In both the Zarnett & Charles experiments and the present tests, the dispersed flow region is replaced by annular flow. This is as expected since at high liquid superficial velocities swirling flow is attained. The centrifugal field then forces the vapor to the central core and the liquid to the tube periphery.

In three of the tests [figures 2(c), 3(a) and (b)], somewhat unusual behavior was observed near the onset of annular flow. Over a narrow range of velocities, the vapor bubbles did not move to the center of the tube but followed the helical path of the ribs at a short distance from the ribs. This flow pattern was designated as "swirl" and is indicated by open squares. Since the vapor bubbles were forced away from the walls, one would expect improved heat transfer characteristics just as in annular flow. The transition from intermittent flow was therefore set at the onset of swirl flow when this flow pattern occurred.

Once what appeared to be annular flow had formed, it was not possible to ascertain from visual observations whether the vapor region was a central core or in an annular ring removed from the center. To determine which situation pertained, a movable probe was used to obtain a series of samples showing the relative volumes of air and water in the flowing fluid stream along the diameter of the tube. The probe consisted of a hollow 0.05 cm dia tube open at one end. Since an isokinetic probe was not used, the samples did not provide quantitative information. However, the qualitative trends can be accepted. The samples clearly showed that the vapor fraction was a maximum in the central region of the tube. It was therefore concluded that the "swirl flow" region was followed by conventional annular flow with a central vapor, or vapor and droplet, core.

Swirling flow was only observed in the swirl and annular flow pattern regions. It will be observed from figures 2 and 3 that, at low and moderate superficial gas velocities, these flow patterns begin at a nearly constant superficial liquid velocity for a given geometry. Thus, a critical superficial liquid velocity is required before swirling flow can be assured for any flow quality.

At liquid velocities below the onset of swirling flow, the flow patterns observed (separated and intermittent flow) in the present tests were essentially the same as those observed in the absence of helical ribs. However, the separated flow region was smaller than that seen with an empty tube.

The change in flow patterns caused by the presence of a single set of helical wires is illustrated in figure 4. This figure compares the flow pattern transitions seen in the same apparatus an empty

5.1 cm tube with those seen in the same diameter tube with helices having two different values of y. It will be observed that, at high gas fractions, annular flow begins at lower gas superficial velocities than in an empty tube. At low and moderate gas fractions, annular flow begins at appreciably lower liquid velocities than the dispersed flow region which it displaces. The intermittent flow region also begins at appreciably lower liquid velocities than in an empty tube.

The flow pattern maps shown in figures 2 and 3(a) were obtained with a single helical wire wound around the periphery of the tube. The flow pattern map in figure 3(b) was obtained with two equally-spaced helical wires in a 2.54 cm tube. The value of y for each wire was approx. 2.5. However, the wire pitch (distance between center lines of two adjacent wires) is only 6.35 cm. Hence, $(P/2D)$ is not equal to y, as when a single wire is used, but equals $y/2$.

The tube diameter, wire diameter and value of y producing the data of figure 3(b) are the same as those used for the tests represented by figure 3(a). Comparison of figure 3(a) and (b) shows that the introduction of a second wire reduces the velocity at which swirl flow begins at low qualities (from $\sim$0.7 to $\sim$0.45 m/s). The velocity at which the intermittent-stratified transition occurs is similarly reduced. The transition to annular flow at high gas velocities is affected very little by the insertion of the second coil.

When the flow pattern maps of the present study are compared with the Zarnett & Charles (1969) map (figure 1), it is seen that Zarnett & Charles did not observe separated flow. In view of the displacement of separated flow to lower velocities as y is reduced, separated flow would be expected at very low superficial liquid velocities for the low y values used by Zarnett & Charles. It appears that the separated flow pattern, if it existed at all, would exist only at liquid velocities below the range of the Zarnett & Charles tests.

An unexplained difference is the bubble flow observed by Zarnett & Charles (1969). In their tests, bubbles flowed along the top of the tube at low gas flow rates and moderate liquid flow rates. In the present tests, only slug flow was observed in this region. It is possible that the difference in rib cross sections (square for Zarnett & Charles, round for present tests) may have been the cause of this variation.

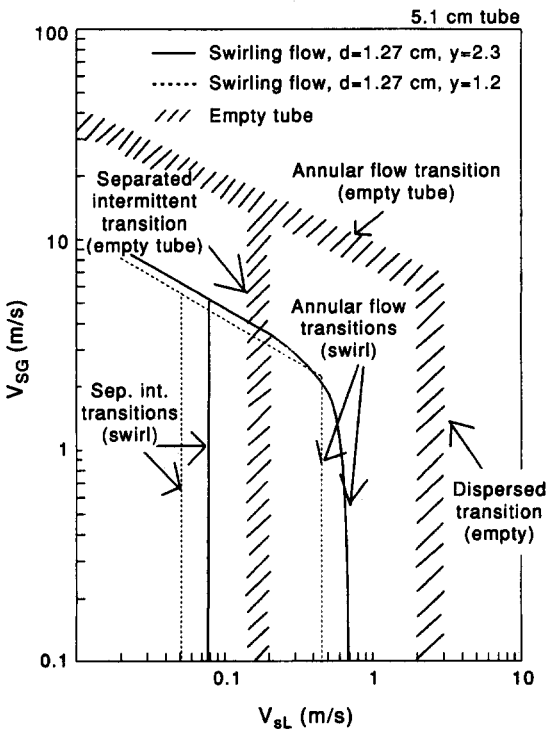

Figure 4. Comparison of flow patterns in an empty tube with those in tubes containing a single wire helix (D = 5.1 cm).

CORRELATION OF FLOW PATTERN TRANSITIONS

While it has been noted that there are some differences between the Zarnett & Charles (1969) flow map and those of the current tests, the onset of annular flow with swirl appears to be consistent in both sets of experiments. It is this annular flow pattern which is desired in order to enhance heat transfer capabilities. Hence, the designer's primary interest in flow patterns would be the determination of the conditions under which swirling annular flow would be present.

Since the annular flow transition occurs at a nearly constant liquid velocity at low gas flows, and at a gas velocity which varies only moderately at high gas flows, separate correlations were devised for each of these regions. A variety of approaches were examined for the low gas flow rate transition line. These included a modification of the approach used by Weisman *et al.* (1979, 1981) for the dispersed pattern in empty tubes. However, this approach was unsuccessful. It was subsequently assumed that the onset of annular flow should be related to the ratio of the vapor drift due to gravity to the relative vapor velocity due to angular acceleration. The drift-flux model of two-phase flow defines the vapor drift velocity, V_{Gj}, as

V_{Gj} = void-weighted average velocity of vapor phase with respect to the velocity of the center-of-volume of the mixture.

Lahey & Moody (1977) suggest that V_{Gj} is flow regime independent and may be calculated from

$$V_{Gj} = k\left[\frac{(\rho_L - \rho_G)\sigma g}{\rho_L^2}\right]^{1/4} \quad [1]$$

where

k = constant
ρ_G, ρ_L = vapor and liquid density, respectively
σ = surface tension
g = gravitational acceleration.

The relative velocity of the vapor, V_r, due to the angular acceleration may be obtained from [1] by replacing g by the radial acceleration "g_R". For a pure liquid flowing through a tube along a helical path, "g_R" is given by (Gambill *et al.* 1961)

$$g_R = \frac{4.6}{D}\left(\frac{V_{SL}}{y}\right)^2 \quad [2]$$

where

V_{SL} = superficial liquid velocity (m/s)
y = helix pitch/2D
D = tube diameter (m).

By assuming that at the onset of annular flow

$$V_r = CV_{Gj} \quad [3]$$

we have at low void fractions

$$C = \left[\frac{4.6}{gD}\left(\frac{V_{SL}}{y}\right)^2\right]^{1/4} \quad [4]$$

or

$$V_{SL} = C'y(gD)^{1/2} \quad [5]$$

A plot of V_{SL} vs $y(gD)^{1/2}$ yielded separate lines for differing values of the ratio of rib height to tube diameter. The data for single helices could be brought together by multiplying $y(gD)^{1/2}$ by $(d/D)^{-0.3}$ where d represents the wire diameter (height for square cross section). The resulting line, however, did not go through the origin. The correlation of the single helix data then has the form:

$$V_{SL} - V_{min} = 0.21y(gD)^{1/2}(d/D)^{-0.3} \quad [6]$$

where $V_{min} = 0.24$ m/s.

It was found that the transition line for the double helix tube could be predicted by the same correlation if "y" was replaced by $P/2D$. (As noted previously, y and $P/2D$ are identical for the single helix but differ by a factor of two for the tube with two helices.) The final correlation for both the single and double helix data was then

$$V_{SL} - V_{min} = 0.21\left(\frac{P}{2D}\right)(gD)^{1/2}(d/D)^{-0.3} \quad [7a]$$

In dimensionless form this becomes

$$\frac{V_{SL} - V_{min}}{(gD)^{1/2}} = 0.21\left(\frac{P}{2D}\right)(d/D)^{-0.3} \quad [7b]$$

The result of using this approach is illustrated in figure 5. The vertical lines through the data points represent the uncertainty in the location of the transition line. The long horizontal bar through the Zarnett & Charles (1969) data point accounts for the fact that their single flow pattern map represented two different values of "y". It may be seen that the agreement obtained is within the uncertainty band for the data.

It was observed that the value of the superficial liquid velocity at which the separated-intermittent transition occurred was related to the onset of annular flow at low gas velocities. The data were brought together by plotting $(V_1 - V_2)$ vs $(p/2D)(gD)^{1/2}$ where

V_1 = superficial liquid velocity at onset of annular flow at low qualities (m/s)
V_2 = superficial liquid velocity at separated-intermittent transition (m/s).

As may be seen in figure 6, the data can be fitted by a straight line, viz,

$$(V_1 - V_2) = 0.24\left(\frac{P}{2D}\right)(gD)^{1/2} + 0.24 \quad [8]$$

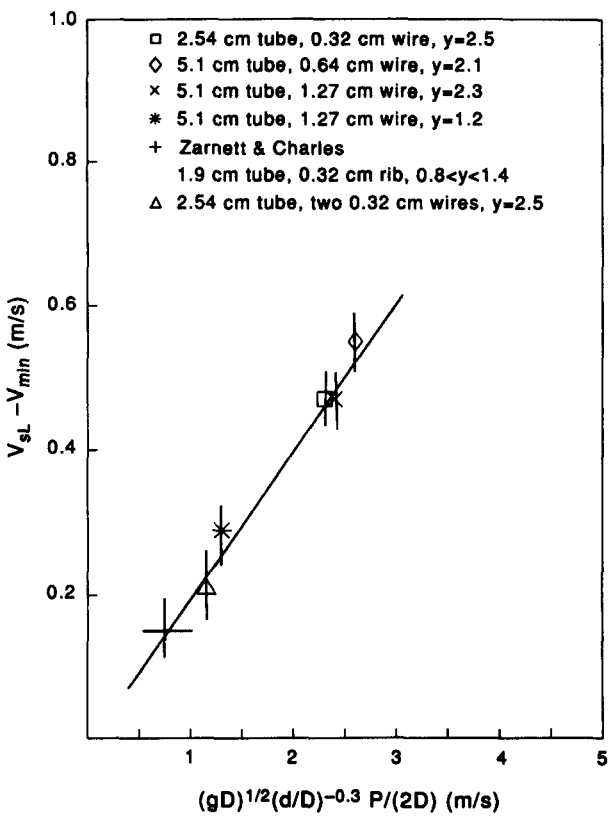

Figure 5. Condition for transition to annular flow at low and moderate void fractions.

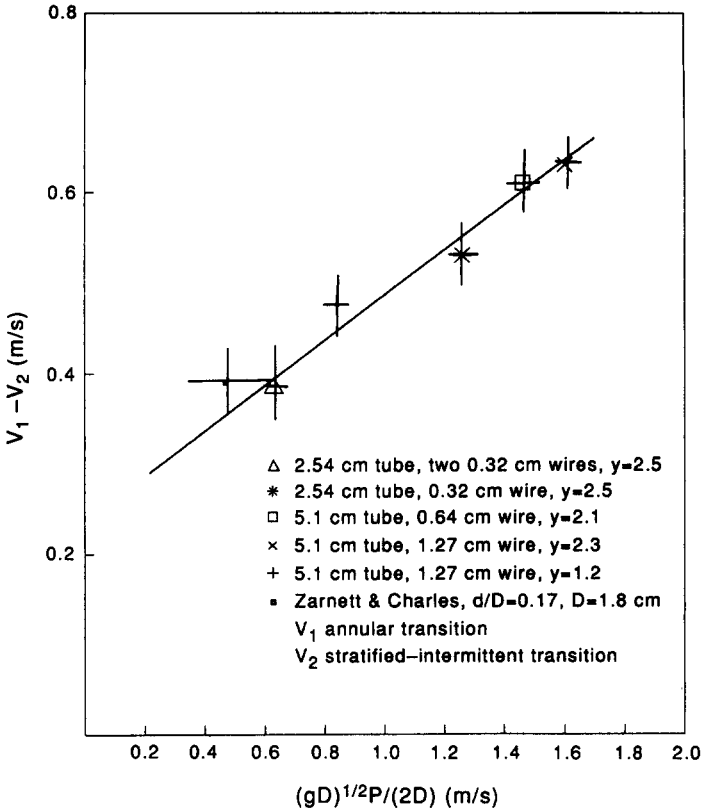

Figure 6. Correlation of separated-intermittent transition conditions.

By combining [7] and [8], we have in dimensionless form

$$V_2/(gD)^{1/2} = \left[0.21\left(\frac{d}{D}\right)^{-0.3} - 0.24\right]\left(\frac{P}{2D}\right) \quad [9]$$

It should be noted that the uncertainty bars in figure 8 have the same meaning as in figure 7.

At high gas flow rates, the onset of annular flow did not seem to be dependent on the value of y. This may be seen in figure 7 where the superficial gas velocity, V_{SG}, at which annular flow begins is plotted vs the ratio (V_{SG}/V_{SL}) for the 5.1 cm tube. The gas velocities at which annular flow begins are significantly below those seen in an empty tube. Data at two different values of y fall on nearly the same line. However, data taken at different values of the rib height, d, fall on different curves. The present data, as well as the results of Zarnett & Charles (1969), fall on the same curve when plotted against (d/D). Within the uncertainty of the data, the transition line for the tube with two helical wires is represented by the same line as for the single helices.

The data are made non-dimensional and tube diameter effects are removed when the transition line data are plotted in terms of the ratio of the superficial gas velocity in a ribbed tube, V_{swirl}, to the superficial velocity in an empty tube, V_{empty}. The results of this approach, shown in figure 8, may be represented by

$$(V_{swirl}/V_{empty}) = 1.1 - 2.42(d/D) \quad [10]$$

Extrapolation of this line to low (d/D) values indicates that helical ribs with a (d/D) value of about 0.04 would have no effect on this flow pattern transition.

It should be noted that the correlations proposed herein appear to apply to ribs of both round and square profiles. However, in view of the limited data available, caution should be used in their application.

AXIAL PRESSURE DROP MEASUREMENTS

The axial pressure drop during two-phase flow is of considerable importance to the designer as this loss determines the pumping power required. Axial pressure drop measurements were

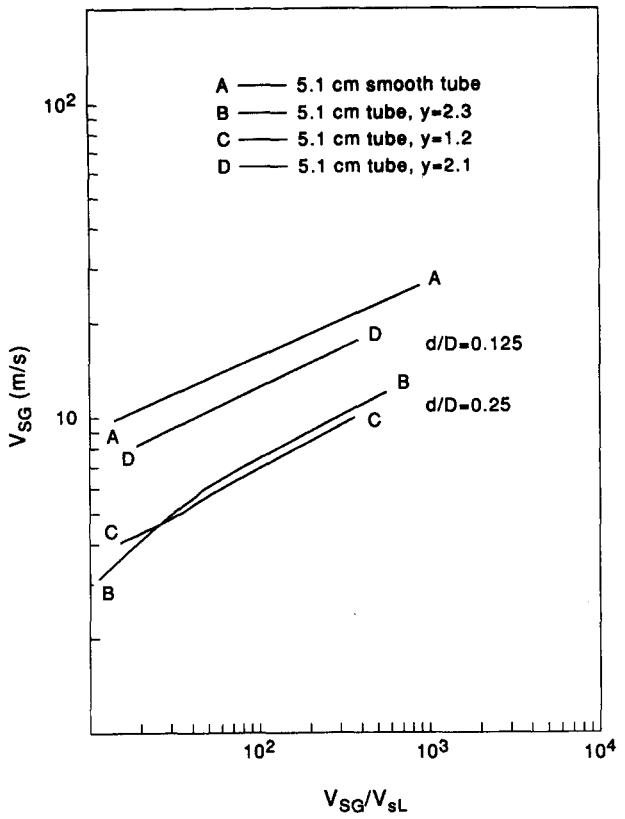

Figure 7. Onset of annular flow at high void fractions.

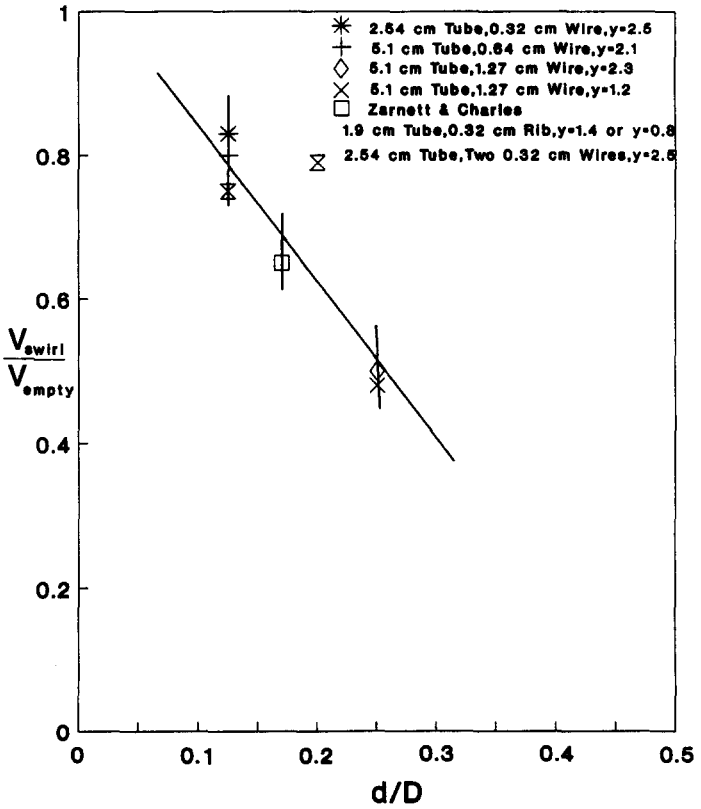

Figure 8. Correlation of transition to annular flow at high void fractions.

attempted in each of the geometries studied. However, in the first geometry studied we attempted to measure the pressure drop across a 240 cm length of the test section. It was found that the variations in rib pitch between the beginning and end of this length were large enough to change the radial pressure profile sufficiently so that meaningful pressure drop measurements were not possible. In the remaining 5.1 cm geometries, axial pressure drops were measured across a 30 cm length over which there were negligible changes in rib pitch. In the 2.54 cm tube, where the pressure drop was high, the pressure drop was measured across a 13 cm length.

Observations at different axial locations indicated the static pressure at the wall, due to the centrifugal field, varied with distance from the helical rib. It was therefore necessary to locate the upstream and downstream wall taps so that they both had approximately the same relative position with respect to a rib. This was possible for the 5.1 cm geometries but not for the 2.54 cm tube. The measurements for the 2.54 cm tubes were obtained by using two movable probes with taps positioned at the center of the flow tube. Each probe consisted of a hollow 0.05 cm diameter tube which was sealed at one end had a 0.02 cm hole facing downstream. Pressure drop measurements from movable probes in the 5.1 cm tube yielded the same results as obtained from the wall taps.

Prior to the measurement of two-phase pressure drops, single phase pressure losses were determined. The Darcy–Weisbach friction factors computed from these data are shown in figure 9 for the various configurations examined. The friction factor predictions obtained from the empirical correlation of Ravigurajan & Bergles (1985) are also shown. Their correlation is given by

$$f_a/f_i = \left\{1 + \left[29.1\ \mathrm{Re}^{(0.67 - 0.06P/D - 0.49\alpha/90)}(\alpha/90)^{(4.59 + 4.11 \times 10^{-6}\mathrm{Re} - 0.15P/D)} \times (P/D)^{(-1.66 \times 10^{-6}\mathrm{Re} - 0.33\alpha/90)}(d/D)^{(1.37 - 0.157P/D)} \times \left(1 + \frac{2.94}{n}\right)\sin\beta\right]^{15/16}\right\}^{16/15} \quad [11]$$

where

f_a = friction factor in internally ribbed tube
f_i = friction factor in smooth tube
Re = Reynolds number
P = rib pitch (distance between adjacenet ribs)
α = helix angle of rib (deg) = $\tan^{-1}(\pi D/P)$

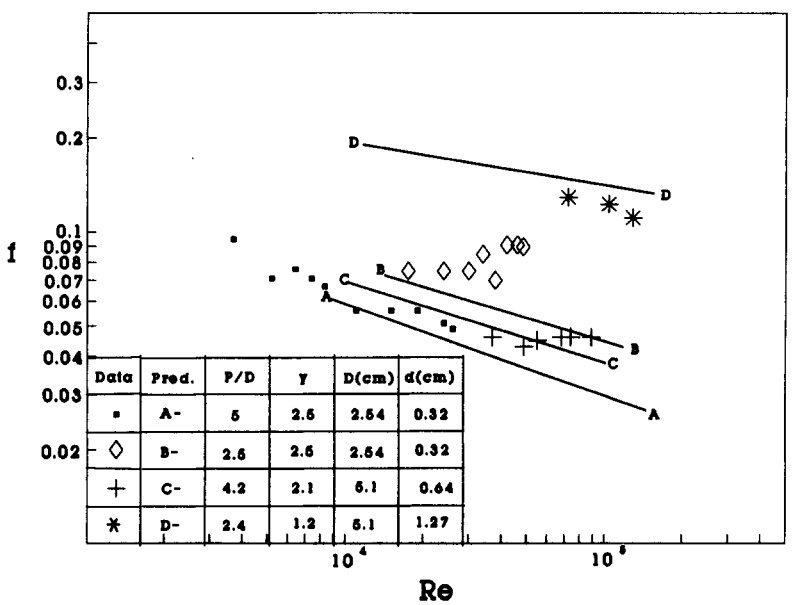

Figure 9. Single-phase friction factors for tubes with a single helix (predictions based on Ravigurajan & Bergles 1985).

β = contact angle of profile (deg)
n = number of sharp corners of rib which face flow (two for triangular and rectangular ribs, infinity for smooth profile).

In the present tests, α varied from 30° to 50° and $\beta = 90°$.

As may be seen from figure 9, moderate agreement between observations and predications is obtained for the single helices with a (d/D) value of 0.125 (curves A and C). The data for the single helix with a (d/D) value of 0.25 lie slightly below the prediction of curve D. The data for the double helix are close to curve B at the lower Reynolds numbers but lie above the predictions at higher Reynolds numbers. The overall agreement of the measurements with the predictions is probably reasonable since some of the original data correlated by Ravigururajan & Bergles (1985) vary by more than a factor of two from the prediction.

Zarnet & Charles (1969) treated their two-phase axial pressure drop data in a manner similar to that used by Lockhart & Martinelli (1949) for empty tube pressure drop. Zarnett & Charles correlated their data by defining ϕ_R^2 where

$$\phi_R^2 = (dp/dz)_{2\phi R}/(dp/dz)_{1\phi R} \quad [12]$$

and

$(dp/dz)_{2\phi R}$ = two-phase presure drop in ribbed tube
$(dp/dz)_{1\phi R}$ = single phase pressure drop in ribbed tube with liquid flowing alone.

Zarnett & Charles (1969) plotted their data vs X, the Martinelli parameter, where X is defined as

$$X = \left[\left(\frac{1-x}{x}\right)^{1.8}\left(\frac{\rho_G}{\rho_L}\right)\left(\frac{\mu_L}{\mu_G}\right)^{0.2}\right]^{1/2} \quad [13]$$

and

x = quality
ρ_G, ρ_L = vapor and liquid densities, respectively
μ_G, μ_L = vapor and liquid viscosities, respectively.

It was found that a plot of X vs ϕ_R^2 yielded a straight line in logarithmic coordinates. The values of ϕ_R^2 they found were slightly somewhat below the two-phase pressure drop multipliers determined by Lockhart & Martinelli for empty tubes.

Figure 10 shows the axial pressure drop data of the present study treated in the same manner as suggested by Zarnett & Charles (1969). It may be seen that the present data behave similarly to those of Zarnett & Charles. The logarithmic coordinate plots show a linear relationship between ϕ_R^2 and X.

Figure 10 also shows the ϕ^2 values obtained by Lockhart & Martinelli for empty tubes. The present data lie on lines which are parallel to the L & M smooth tube correlation. Data from two of the configurations lie at or above the smooth tube line while two configurations fell below the smooth tube predictions.

Most two-phase pressure drop studies, subsequent to those of Lockhart & Martinelli (1949), indicate a mass flux dependence of the two-phase multiplier.

Chisholm & Sutherland (1969–1970) correlated much of the later data by

$$\phi_L^2 = 1 + (c/X) + (1/X^2) \quad [14]$$

where

$\phi_L^2 = (dp/dz)_{2\phi}/(dp/dz)_{1\phi}$
$(dp/dz)_{2_\phi}$ = two-phase pressure drop in smooth tube
$(dp/dz)_{1\phi}$ = single-phase pressure drop in smooth tube with liquid flowing alone
C = empirical constant varying with mass velocity and fluid properties.

The ϕ^2 valued obtained from the Chisholm & Sutherland (1969–1970) correlation for two mass fluxes, which are near the upper and lower limits of the data range, are also plotted in figure 10. It is again seen that observations are both above and below smooth tube predictions.

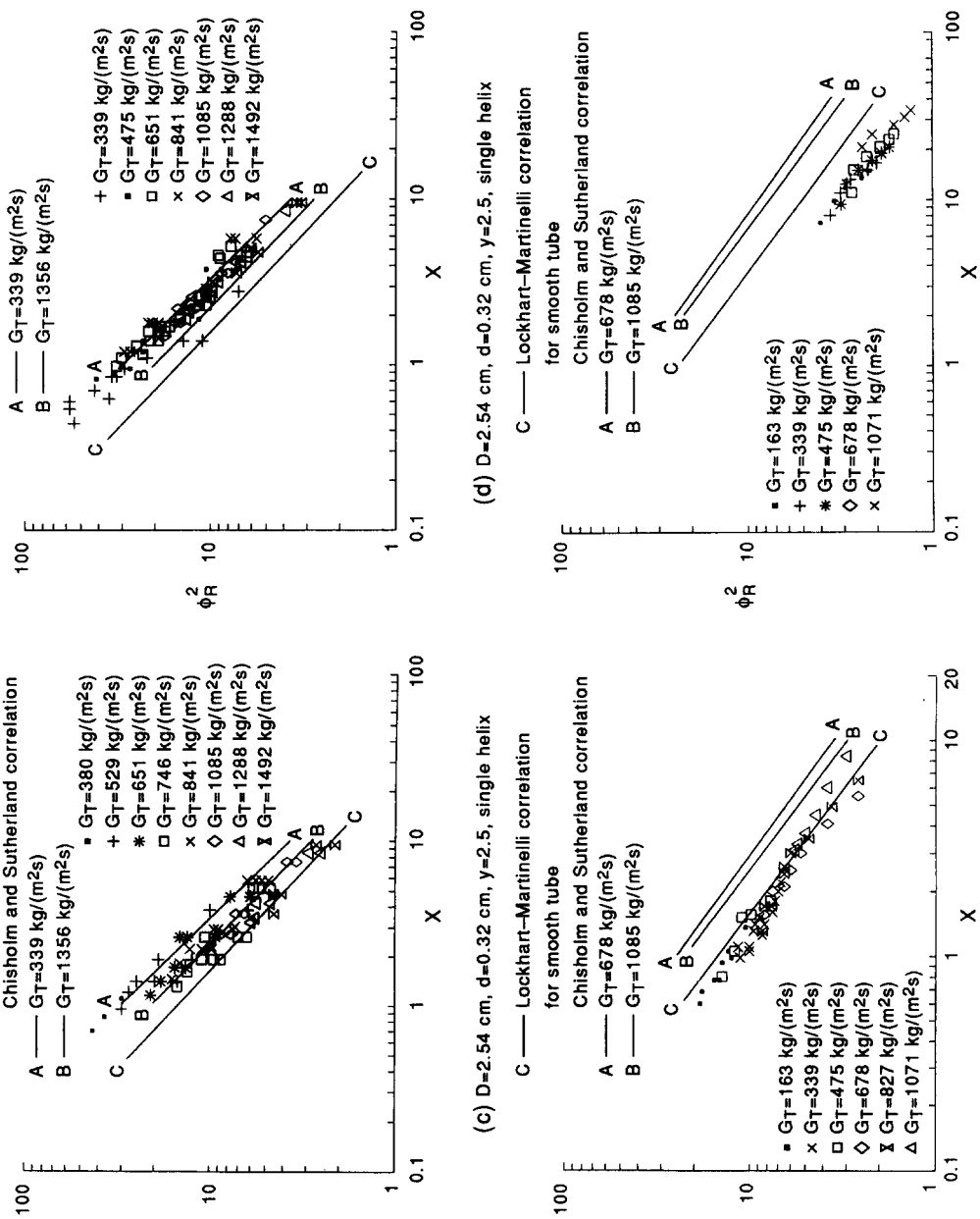

Figure 10. Two-phase multiplier for axial pressure drop in tubes with a wire helix.

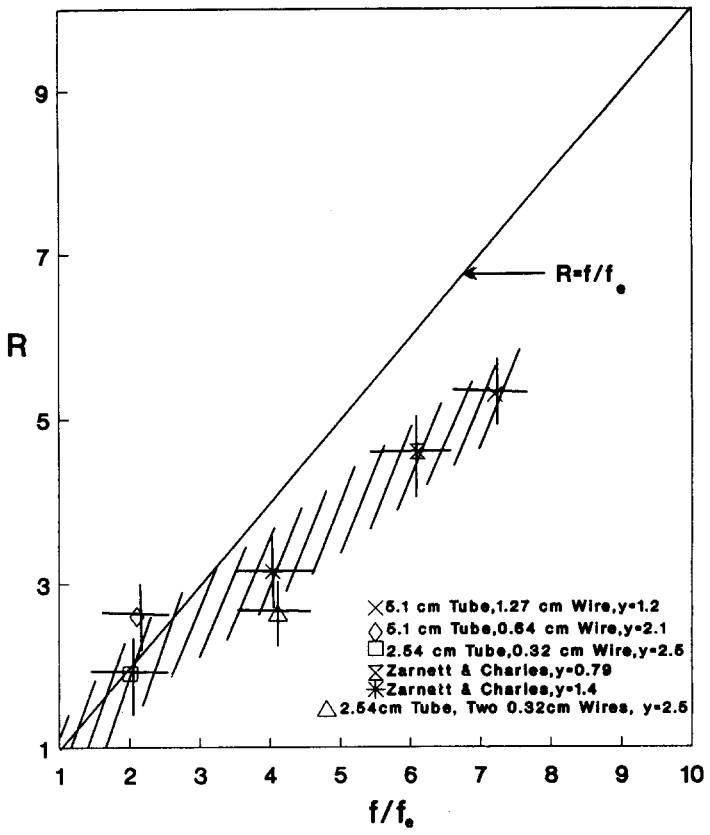

Figure 11. Ratio of two-phase pressure drop in a ribbed tube to two-phase pressure drop in an empty tube.

Lockhart & Martinelli values for ϕ_L^2 in smooth tubes were chosen as the standard to which the present data would be compared. This selection was made since: (a) the L & M values of ϕ_L^2 were also obtained with air and water; (b) the present data show little mass flux dependence and the L & M ϕ_L^2 values are not dependent on mass flux; and (c) the present data lie on lines which are essentially parallel to the ϕ^2 *vs* X prediction line for smooth tube data.

The present data and the Zarnett & Charles (1969) data, were represented by lines through the means of the various data sets. Since these lines are parallel to the L & M prediction, each data set may be represented by a single ratio of ϕ_R^2 to ϕ_L^2. Initial efforts to correlate this ratio were unsatisfactory. A revised approach was therefore developed by defining the quantity R which represents the ratio of two-phase pressure drop in a helically ribbed tube to the two-phase pressure drop in an empty tube. This parameter is computed from:

$$R = (\phi_R^2/\phi_L^2)(f/f_e) \qquad [15]$$

where

f = single-phase friction factor for tube containing wire helix
f_e = single phase friction factor for empty tube.

Since the ratio (f/f_e) varies little with Reynolds number, and (ϕ_R^2/ϕ_L^2) is a constant for a given configuration, the parameter R is also approximately constant for a given configuration.

Figure 11 shows the average values of R, obtained from the present tests and computed from the data of Zarnett & Charles (1969), as a function of (f/f_e). When plotted in this manner, the data from the two sets of tests are roughly consistent. The data appear to indicate that, for (f/f_e) values below about 2.25, R is roughly equal to (f/f_e). However, at values of (f/f_e) above about 3.5, R is only about 70% of the value of (f/f_e). Although the data point for the double helix lies slightly

below the band through the single helix data, there are insufficient data to determine whether this is significant or is the result of data scatter.

CONCLUSION

Additional data on both two-phase flow patterns and pressure drop in helically ribbed tubes have been obtained. When these data are considered along with the earlier Zarnett & Charles (1969) data, it is possible to develop preliminary correlations for predicting the onset of swirling annular flow. The flow pattern transition data can be confidently used for air–water systems flowing in tubes with diameters between approx. 1 and 5 cm and where $0.1 < V_{SL} \leqslant 5$ m/s, $0.2 < V_{SG} < 25$ m/s. The applicability of these correlations to systems other than air–water remains to be determined.

The data from the present tests also allow the approximate estimation of two-phase pressure drop in helically ribbed tubes. Additional data are obviously needed to allow the effects of physical properties and different geometric conditions to be incorporated in a definitive correlation.

The flow pattern data indicate that if swirling annular flow is to be maintained in a boiler tube at all qualities, the inlet liquid velocity must exceed a geometry-dependent minimum value. One would expect that enhanced heat transfer would not be obtained from ribbed tubes unless operation is above this minimum liquid velocity. This supposition is supported by the data of Watson *et al.* (1974). In their critical heat flux studies, they found little difference between the performance of a smooth and ribbed tube until a critical mass flux was exceeded. Once this occurred, a pronounced increase in the critical heat flux was observed. However, the mass flux at which this improvement occurred was appreciably above the value which would be obtained from the correlations presented here. This is not surprising considering the vastly different physical properties of high pressure steam–water mixtures and the low pressure air–water mixtures of the present tests. It is clear that experiments utilizing high density vapor are needed.

A question which also remains to be answered is the determination of the conditions under which dispersed flow is not replaced by annular flow. For large values of "y" and very small rib heights, one would expect that the ribs would not be effective in producing annular flow at low void fractions. Based on previous studies in smooth and artificially roughened tubes (Weisman *et al.* 1988), dispersed flow occurs when

$$\left\{\frac{|\mathrm{d}p/\mathrm{d}z|_{Lo}}{(\rho_L-\rho_G)}\right\}^{1/2}\left[\frac{\sigma}{(\rho_L-\rho_G)g_0D^2}\right]^{-0.22} \geqslant 1.5 \qquad [16]$$

where

$|\mathrm{d}p/\mathrm{d}z|_{Lo}$ = absolute value of single phase pressure drop with entire mass flowing as liquid
σ = surface tension.

For a given geometry and liquid–vapor pair, this predicts that the dispersed flow transition occurs at a nearly constant liquid mass flux at low and moderate void fractions. It would seem reasonable to suppose that, if the mass flux predicted for the onset of dispersed flow by [16] is less than the mass flux obtained for the onset of annular flow from [7], a region of dispersed flow would exist. It is not clear whether the dispersed region would then give way to annular flow at higher mass fluxes or whether annular flow would fail to appear at all.

Another question which needs to be considered is the degree of applicability of the flow pattern transition correlations deduced from lines containing wire helices to metallic tubes in which the ribs have been produced by machining or drawing. Since industrial boiler tubes are all of the latter category, the question has considerable significance. While the same flow patterns are expected, the transitions lines may show somewhat different behavior.

REFERENCES

CHISHOLM, D. & SUTHERLAND, L. A. 1969–1970 Predication of pressure gradients in pipeline systems during two-phase flow *Proc. Inst. Mech. Engrs.* **184,** 24.

GAMBILL, W. R., BUNDY, R. D. & WANSBROUGH, R. W. 1961 Heat transfer, burnout and pressure drop for water in swirl flow through internal tubes with twisted tapes. *Chem. Engng Prog. Symp. Ser.* **32,** 127.

LAHEY, R. T. & MOODY, F. J. 1977 *The Thermal-hydraulics of a Boiling Water Nuclear Reactor*, 1st edn, p. 204. American Nuclear Society, LaGrange Park, IL.

LOCKHART, R. W. & MARTINELLI, R. C. 1949 Proposed correlation of data for isothermal two-phase two-component flow in pipes. *Chem. Engng Prog.* **45,** 39.

RAVIGURURAJAN, T. S. & BERGLES, A. E. 1985 General correlation of pressure drop and heat transfer for single phase turbulent flow in internally ribbed tubes. In *Augumentation of Heat Transfer in Energy Systems* (Edited by BISHOP, P. J.), *ASME Proceedings of Heat Transfer Div.*, Vol. 52.

WATSON, G. B., LEE, R. A. & WEINER, M. 1974 Critical heat flux in inclined vertical smooth and ribbed tubes. *Proc. 5th Engng Heat Transfer Conf.*, Tokyo, Japan, Paper 6.8 Japanese Society of Mechanical Engineering.

WEISMAN, J., BEHBAHANI A. & BHATTACHARYA, S. 1988 An improved representation of the dispersed flow transition. In *Particulate Phenomena and Multiphase Transport* (Edited by VEZIROGLU, T. N.). Hemisphere, Washington, DC.

WEISMAN, J., DUNCAN, D., GIBSON, J. & CRAWFORD, T. 1979 Effects of fluid properties and pipe diameter on two-phase flow patterns in horizontal lines. *Int. J. Multiphase Flow* **5,** 417.

WEISMAN, J. & KANG, S. Y. 1981 Flow pattern transitions in vertical and upwardly inclined lines. *Int. J. Multiphase Flow* **7,** 271.

ZARNETT, G. D. & CHARLES, M. E. 1969 Cocurrent gas–liquid flow in horizontal tubes with internal spiral ribs. *Can. J. Chem. Engng* **47,** 238.